

The Use of Macro-Fiber Composites for Pipeline Structural Health Assessment

Andrew B. Thien¹, Heather C. Chiamori², Jeff T. Ching³, Jeannette R. Wait⁴, and Gyuhae Park⁴

¹Dept. of Mechanical Engineering, Univ. of Cincinnati, Cincinnati, OH 45220

²Dept. of Mechanical Engineering, Univ. of California Berkeley, Berkeley, CA 94720

³Dept. of Civil Engineering, Univ. of California Irvine, Irvine, CA 92697

⁴Engineering Sciences & Applications, Los Alamos National Laboratory, Los Alamos, NM 87545

ABSTRACT

Pipeline structures are susceptible to cracks, corrosion, and other aging defects. Implementation of a real-time damage diagnostic system for pipeline structures can reduce operational and maintenance costs. This research investigates coupled impedance-based and Lamb wave propagation methods that can be simultaneously used for overall pipeline structural health monitoring (SHM). Self-sensing impedance measurements are used to detect damage occurring at pipeline connection joints, while the Lamb wave propagation measurements identify cracks and corrosion along the surface and through the thickness of the pipe structure. These techniques utilize the electromechanical coupling effects of piezoelectric-based active sensors. For this study, the small, non-intrusive, and flexible Macro-fiber composite (MFC) patches are used as both sensors and actuators. The electrical impedance signatures from MFC sensors are recorded before and after induced damage. The location of joint damage is successfully determined from the measured responses. For the Lamb wave propagation analysis, a ring of MFC patches, which were used for the impedance method, generates high frequency Lamb waves that travel through the structure. Both wave attenuation and reflection features are used to identify cracks or corrosion damage along the main body of the pipeline. Based on the success of this project, guidelines for full-scale development of low-cost, active-sensing based diagnostic techniques suitable for piping systems are presented.

Nomenclature

a	geometric constant of material of piezoelectric materials
d_{3x}	sensor coupling constant at a neutral state
$F(m, n)$	flexural non-axially symmetric modes with harmonic number of circumferential variation and index counter
$L(m, n)$	longitudinal axially symmetric modes with index counter
$T(m, n)$	torsional axially symmetric modes with index counter
$Y(\omega)$	electrical admittance
Y_{xx}^E	complex Young's modulus with a zero electric field
Z_a	sensor mechanical impedance
Z_s	host structure mechanical impedance
ϵ_{33}^T	dielectric constant at a neutral state
ρ	Correlation coefficient
$Z_{i,1}$	Baseline impedance data at frequency i
$Z_{i,2}$	Compared impedance at frequency i
\bar{Z}_1	Mean of signal
σ	Standard deviations

1. INTRODUCTION

Several issues emphasize the importance of developing and implementing a real-time, structural health monitoring (SHM) system for pipeline structures. First, the ability to quickly and accurately evaluate the condition of a pipeline structure after a natural disaster, such as an earthquake, is critical to uninterrupted plant or facility operation as well as maintaining the safety and well-being of workers and nearby residents. Delays in assessment of a potentially damaged pipeline could result in fire hazards caused by ruptured gas pipelines or shutdowns of hospital critical care facilities. Another reason to pursue a robust pipeline health monitoring system involves reduction of operational and maintenance costs. Maintenance inspections often involve expensive equipment for non-destructive evaluation of pipeline structures. Shutting down an entire plant or sections to perform SHM is expensive, time-consuming, and reduces plant efficiency and production capabilities. Several documented gas pipeline accidents have resulted because of problems with detecting pipeline damage [1,2]. The United States obtains approximately 30% of its total energy consumption from natural gas, and millions of miles of pipelines exist to transport the natural gas. These are compelling reasons to implement a real-time, health monitoring system that could accurately determine the health of a pipeline network [3].

If a well designed, structural health monitoring system were in operation, it is evident that one could reduce the maintenance cost and avoid catastrophic failure associated with pipeline structures. A promising technology for pipeline structural health monitoring involves the use of piezoelectric materials, such as Lead Zirconate Titanate (PZT). The electromechanical coupling effect of PZT establishes a relationship between the electrical and mechanical domains. As a result, PZT experiences a mechanical strain when an electric field is applied, and conversely, PZT produces an electric charge when stressed mechanically. The coupling property allows PZT transducers to perform both actuation and sensing in a structural health monitoring system. When bonded to a structure, the PZT wafer can be used to excite the system at high frequencies, utilizing the high-bandwidth capability of the PZT material, and then measure corresponding structural responses. Examples of documented success using PZTs in the areas of SHM are impedance-based structural health monitoring methods [4,5,6], Lamb wave propagations [7,8], and the integrated use of those two methods [9,10], which is the subject of this paper.

In this study, piezoelectric Macro-Fiber Composite (MFC) patches are used for the development of a real-time, low cost, structural health monitoring system for pipeline structures. The advantages of using PZT for SHM include low cost, light-weight, low-power consumption, non-intrusive, and high bandwidth that allow the detection of incipient-type damage. Additional advantages are obtained through the use of MFC patches, including high flexibility and extreme durability compared to the piezoceramic counterpart [11,12,13]. The flexibility of MFC patches is particularly useful to pipeline monitoring because the curved surface of the pipe may be used as an application site.

This research focuses on damage identification in the flanged joint connections and main body of a pipeline using MFC patches to both excite the structure and measure the resulting responses. To simulate damage at the pipe joint connections, bolts are removed from the flanges and the location is identified from the analysis of impedance methods. Corrosion damage was simulated with the use of pipe clamps attached to the main body of the pipeline. The location of corrosion damage is determined from the analysis of Lamb wave propagations. The theory supporting these techniques, experimental procedures and results are detailed in the following sections.

2. BACKGROUND

2.1 Impedance Method

Based on the work of Sun, et al. [14], the impedance-based monitoring technique is used to monitor real-time changes in the mechanical impedance of a structure. Compared with initial measurements, a damaged structure will exhibit changes in its stiffness and damping characteristics which affect its mechanical impedance. Because direct measurements of the mechanical impedance of a structure are difficult to obtain, the electromechanical coupling effect of PZT materials is utilized. Any subsequent damage to a host structure will result in changes to its mechanical impedance, which will be observed by changes in the electrical impedance of the PZT materials.

In this experiment, the MFC patch acts as both an actuator and a sensor when obtaining the impedance signature from a structure. An alternating electric field is applied to the MFC patch, creating high frequency excitations in

the host structure. At high frequencies, a dynamic response of the host structure is generated only in an area local to the patch which is then measured by the MFC sensor as an electrical response. The relationship between the host structure's mechanical impedance and the electrical impedance of the MFC patch is represented by the following equation [14]:

$$Y(\omega) = \frac{I}{V} = i\omega a \left(\bar{\epsilon}_{33}^T - \frac{Z_s(\omega)}{Z_s(\omega) + Z_a(\omega)} d_{3x}^2 \hat{Y}_{xx}^E \right) \quad (1)$$

where Y is the electrical admittance or the inverse of the electrical impedance, a is the PZT material's geometric constant, $\bar{\epsilon}_{33}^T$ is the dielectric constant at a neutral state, Z_a is the PZT's mechanical impedance, Z_s is the host structure's mechanical impedance, d_{3x} is the PZT coupling constant at a neutral state, and \hat{Y}_{xx}^E is the PZT's complex Young's modulus with a zero electric field. Because all parameters except Z_s , the host structure's mechanical impedance, are properties of the PZT material, only the mechanical impedance of a structure uniquely defines the electrical impedance of the PZT transducer. As a result, the electrical impedance signature of the PZT material can measure changes in the host structure's mechanical impedance. For additional information regarding impedance methods, refer to [4,5,6].

For this study, two frequency ranges are examined: 50-60 kHz and 110-120 kHz. At frequencies greater than 30 kHz, the dynamic response of a host structure is limited to local areas surrounding the MFC patch. Additionally, high frequency excitation allows measurements obtained by the MFC patch to be insensitive to far-field conditions such as mass-loading and boundary conditions. An advantage of this limited sensing area is that the method not only detects the presence of damage but can also pinpoint which flange is damaged.

For the impedance method, a scalar damage metric is used to interpret and quantify the variations of measured responses. The damage metric is defined in this study as cross-correlation coefficients [4]. The degree of linear relationship between baselines and in-question measurements can be assessed with cross-correlation coefficients. For the impedance method, only the real component of the impedance measurement is considered due to its greater sensitivity to damage [4]. The visual interpretation of the scalar damage metric is based on comparison with baseline values. Large increases in the scalar damage metric indicate the occurrence of damage. Threshold values would depend on the application site, type of piping structures, and other environmental factors [15].

2.2 Lamb Wave propagation Method

Much effort has been directed toward the use of Lamb wave propagation as a structural health monitoring tool in plates, hollow cylinders, such as pipes, and other complex structures. Lamb waves are useful for corrosion detection because the waves are sensitive to surface and internal damage and propagate over long distances, which is especially useful for pipe structures [16]. Lamb waves are mechanical waves that have wavelengths on the same order of magnitude as the thickness of a structure and occur as an infinite number of discrete modes [17]. These modes occur when longitudinal and shear wave reflections constructively interfere and energy propagates through the plate [17].

Monitoring pipe structures using Lamb waves is complicated by several factors. Generating a single, pure mode for a pipe structure is difficult due to the presence of multiple modes at each frequency [18], whereas an isotropic plate structure has only two distinct modes, symmetric and anti-symmetric, present at lower frequencies. Nomenclature for the three classes of tube modes present in hollow cylinder wave guides are outlined by Silk and Bainton [17], then modified by Demma, et al. [19] for their software, referred to as *Disperse*. The three types of modes are as follows: Longitudinal axially symmetric modes $L(0,n)$; Torsional axially symmetric $T(0,n)$; and Non-axially symmetric (Flexural) modes $F(m,n)$. The first two classes correspond to modes in a flat plate. For this notation, m represents the harmonic number of circumferential variation and n is an index counter [19]. Another difficulty with Lamb wave techniques, in general, is that the modes are dispersive. The shape of the propagating wave will change with distance which makes interpretation of results somewhat difficult [18].

Recent research works [16,18,19,20] have shown significant success with pipeline structural health monitoring, including the development of software to determine cylindrical shell mode diagrams, portable rings of transducers

for attachment to the outside of a pipe, and commercially viable monitoring products using Lamb wave propagation as a tool for damage detection. These techniques use a pulse-echo transducer arrangement, where arrival times and changes in signal amplitude at reflection are used to indicate the presence and location of defects [21]. The ring consists of independent transducers distributed evenly about the pipe circumference [16].

For this research, the Lamb wave technique is examined with the use of directional MFC patches instead of a dry-coupled PZT ring transducer assembly. As discussed in the introduction, the advantages of using MFC patches are the flexibility of the patch allowing direct mounting to the curved surface of the pipe, inexpensive fabrication methods that reduces overall cost of the sensors, and the directionality of the signal generation by a ring of MFC patches that excites axisymmetric modes while minimizing flexural modes. The technique first involves selection of a narrow frequency bandwidth for good signal strength and limited dispersion over long distances [16]. Second, spatial selectivity of transducers depends on the number of modes present in the selected frequency signal range.

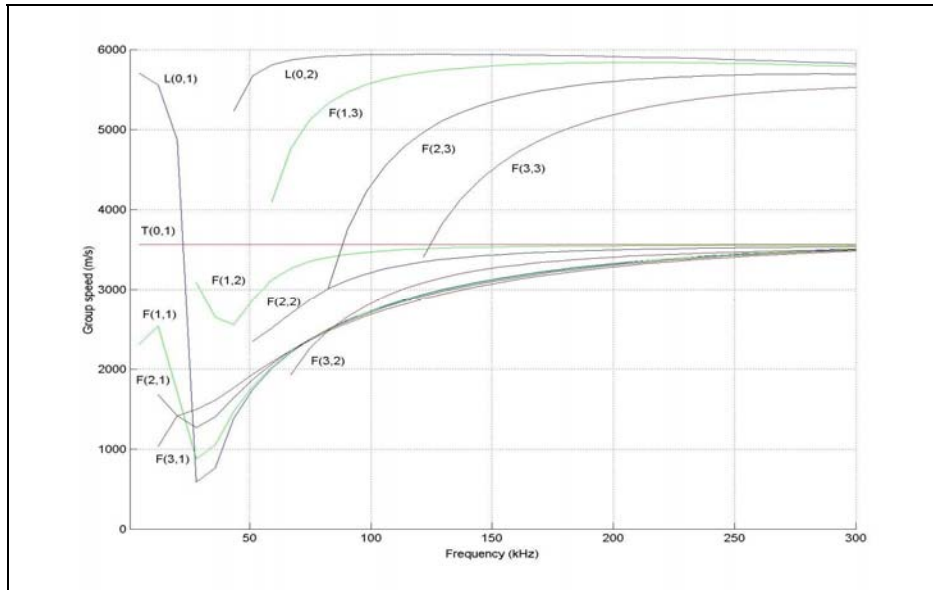


Figure 1: Group velocity curves for pipeline structure

As shown in Figure 1, multiple modes exist at any given frequency. Figure 1 was generated using the *PCDISP* software [22]. To successfully use Lamb wave propagation as a tool for detecting and locating structural damage in pipelines, a carefully designed excitation frequency must be chosen. Ideally, a single mode would be excited so that the measured responses would be easily identified and interpreted. A group velocity dispersion curve is generated for the pipeline structure from the pipe structure geometric and material properties. For this experiment, mode $L(0,2)$ is chosen as the best candidate for excitation due to its relative non-dispersive group velocity characteristic over a large frequency range [18]. As shown in Figure 1, mode $L(0,2)$ is the fastest of the modes in the given frequency range. The $L(0,2)$ mode will arrive at the MFC sensor first and can be separated from other signals if time-domain gating is used. A 70-kHz frequency is selected from the group velocity curve because $L(0,2)$ has good separation from $F(1,3)$ and other modes. At 70-kHz, nine flexural modes exist. According to Alleyne et al. [18], the ideal number of transducers in the ring array should be greater than the number of flexural modes. For this experiment, however, only four transducers were used due to geometric (size of MFC patch) limitations. Further research will incorporate more transducers.

Once baseline measurements of the pipeline are recorded, comparison with subsequent measurements involving simulated damage should show changes in wave reflection and attenuation of the input signal. The selection of a frequency where the mode is the fastest and least-dispersive allows time-of-flight data to be used to determine the presence and location of damage.

3. EXPERIMENT

3.1 Apparatus

The apparatus used for the experimental procedures was a simple pipeline consisting of three, aluminized steel, pipe sections. The three sections are connected together using two flanged joints to form a continuous, straight pipeline, as seen in Figure 2. The entire apparatus was 3.96-m long. Each flanged joint has four bolts, and each bolt was tightened with a torque wrench to 22.6-N-m. The pipe sections have an outer diameter of 63.5-mm and a wall thickness of 4.8-mm. For the impedance tests, the pipe was suspended using elastic cords. For the Lamb wave tests, it was allowed to rest on the floor.

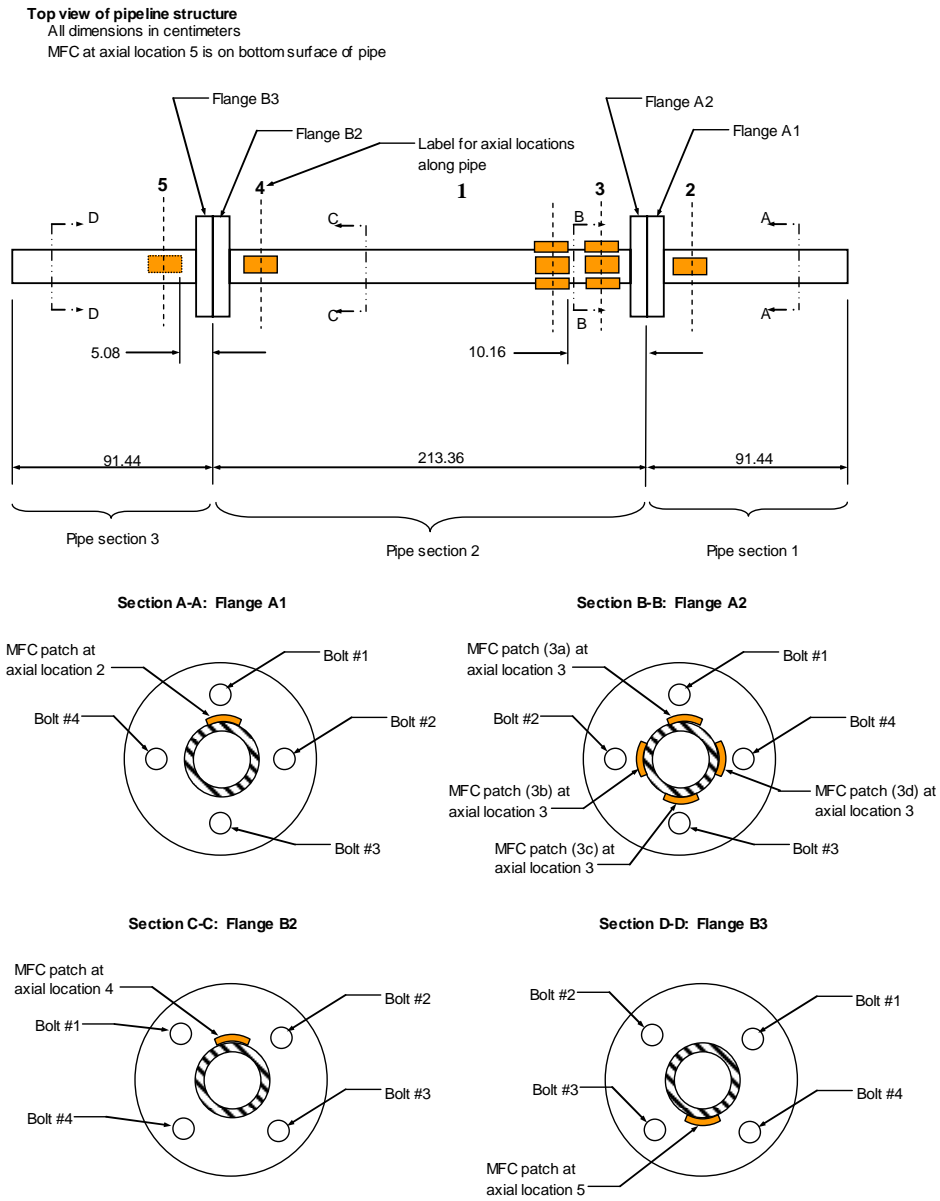


Figure 2: Dimensioned drawing of apparatus

Several MFC patches were used to monitor the condition of the pipeline structure. The MFC provides large flexibility that allows easy integration into the pipeline, as shown in the figure. Traditional piezoceramic materials are not suitable for this application, as confirmed by previous studies. The patches have an active area of 85-mm x 57-mm with overall dimensions 110-mm x 75-mm (Smart-Materials, Inc., M8557). An example of the mounted

patches can be seen in the **Figure 3**. The patches were bonded to the metal surface of the pipe using epoxy, which was allowed to cure in a vacuum bag for 12 hours at a gauge pressure of 1.02-atm. As seen in Figure 2, five axial locations along the length of the pipe were chosen to mount the MFC patches.

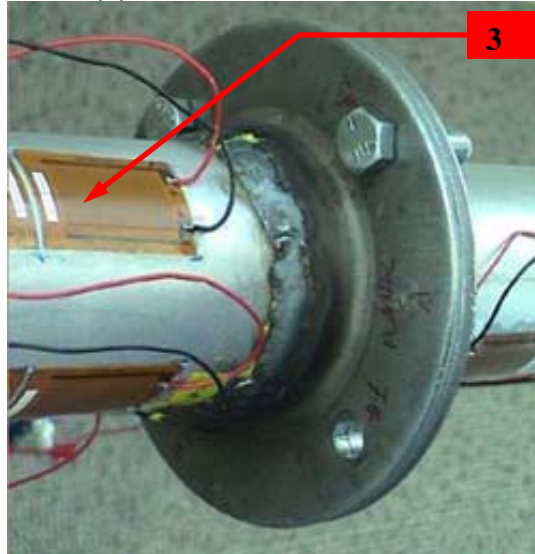


Figure 3: Example MFC patch (3b)

3.2 Procedure

3.2.1 Impedance Method

For the impedance measurements, four MFC patches were used. The pipeline structure, containing all three sections was suspended using two elastic cords. The elastic cords were attached approximately 46-cm from each end of the structure, as seen in Figure 4. An Agilent 4294 impedance analyzer was used for the data acquisition. Two frequency ranges were used for the measurements. The low frequency range was 50 to 60-kHz, and the high frequency range was 110 to 120-kHz. For both frequency ranges, 801 data points were taken. A 1-V swept sine wave was used for the excitation. Four averages were made per point, and only one complete sweep was used.

All impedance data were taken in sets. A set of data contained eight ensembles. Each of the eight ensembles involved measuring the impedance of a given MFC patch for one of the two frequency ranges. An impedance measurement was taken from each MFC located at 2, 3, 4, 5 in figure 2 for both frequency ranges. Therefore, the use of four MFC patches and two frequency ranges corresponded to eight ensembles of data per data set. Five sets of baseline measurements were taken. The purpose of the baseline measurements was to provide a means of comparison between the undamaged and the simulated damaged conditions of the pipeline structure. In an effort to capture potential differences due to environmental changes, the baseline measurements were taken at various times over the course of three days. After that, three damage cases were measured. Each damage case involved removing one or more bolts from a particular flange in an effort to simulate loosening of the flanged joint. For each of the three cases, three sets of data were taken at different times in the day. For the first case, bolt one was removed from flange A (see Figure 2). For the second case, bolts one and two were removed from flange A (see Figure 2). For the third case, bolts one and two were left removed from flange A, as in case two. The pipe was then circumferentially rotated 180-degrees. Since the pipe was suspended at its ends, rotating it 180-degrees reversed the stress on the joint damage from compression to tension. A summary of the measurement cases can be seen in Table 1.

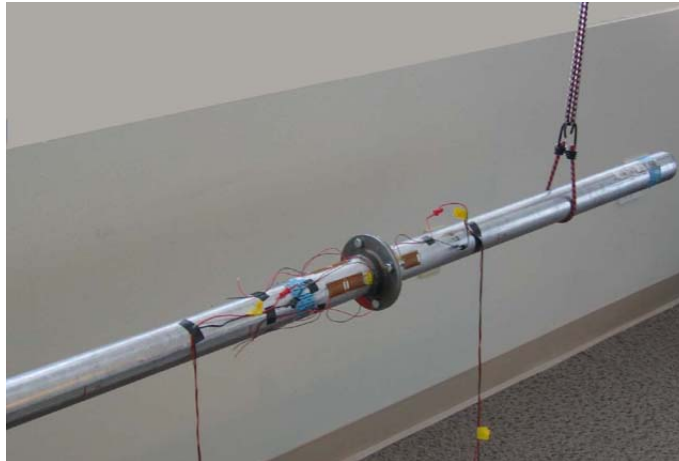


Figure 4: Pipe suspension method

Table 1: Damage cases

Damage case	Description
Case 1	Bolt one removed from Flange A
Case 2	Bolts one and two removed from Flange A
Case 3	Same bolts as Case 2, but pipe rotated 180°

3.2.2 Lamb Wave Method

For the Lamb wave measurements, two circumferential rings of four MFC patches each were used. The two rings were located at axial locations 1 and 3. In other words, only MFC patches *1a*, *1b*, *1c*, *1d*, *3a*, *3b*, *3c*, and *3d* were used. A portable data acquisition system was used to generate the input waveform and measure the subsequent traveled waves. The waveform was amplified by an external power amplifier. The amplified waveform was then simultaneously input to the four MFC patches at axial location 3. The four MFC patches at axial location 1 were then used to simultaneously measure the response. The response signal was sent to an internal 5-V amplifier card, and the data were then stored for analysis. The input waveform was a burst waveform. The burst waveform was created by applying a Gaussian window to a sine wave. The frequency chosen for the waveform was 70 kHz, as explained in the previous section. Damage was simulated by attaching two pipe clamps to the structure. The clamps were located 1.04-m from flange A2.

4. RESULTS

4.1 Impedance Method

An example of an impedance measurement is shown in Figure 5. This figure shows the entire frequency range used in the frequency measurement of 50-60 kHz. The impedances in this figure were taken from MFC 2, which is located closest to flange A. Only the real portion of the electrical impedance is analyzed to predict damage because it is more sensitive to structural changes than the imaginary part. The first three damage cases are plotted in comparison to a baseline measurement. A view of the impedances over a narrower frequency range, 55-57 kHz, can be seen in Figure 6. It can be seen in the figure that as damage increases, corresponding changes in impedance are observed. However, it is difficult from such a plot to quantify the degree to which the structure is damaged. In order to quantify the amount of change in impedance signature due to damage, the damage metric is calculated.

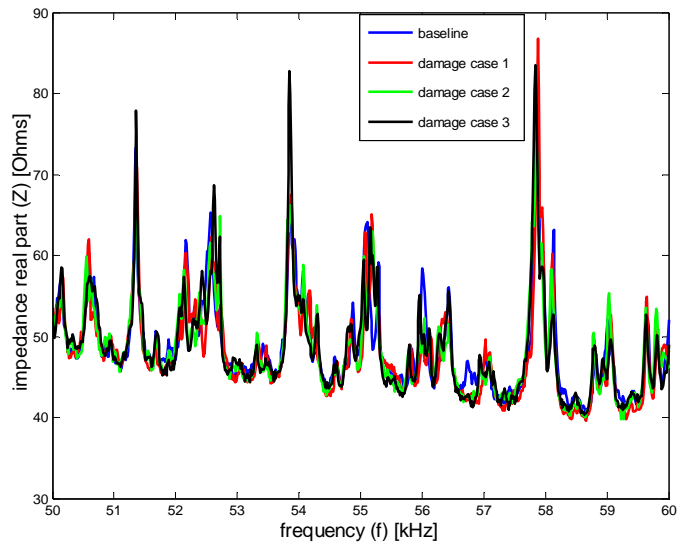


Figure 5: Comparison of baseline and damage-case impedances (50 to 60-kHz)

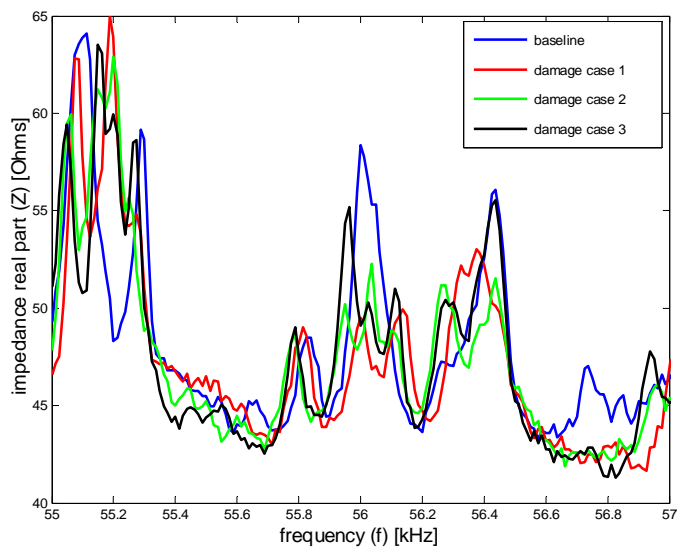


Figure 6: Comparison of baseline and damage-case impedances (55 to 57-kHz)

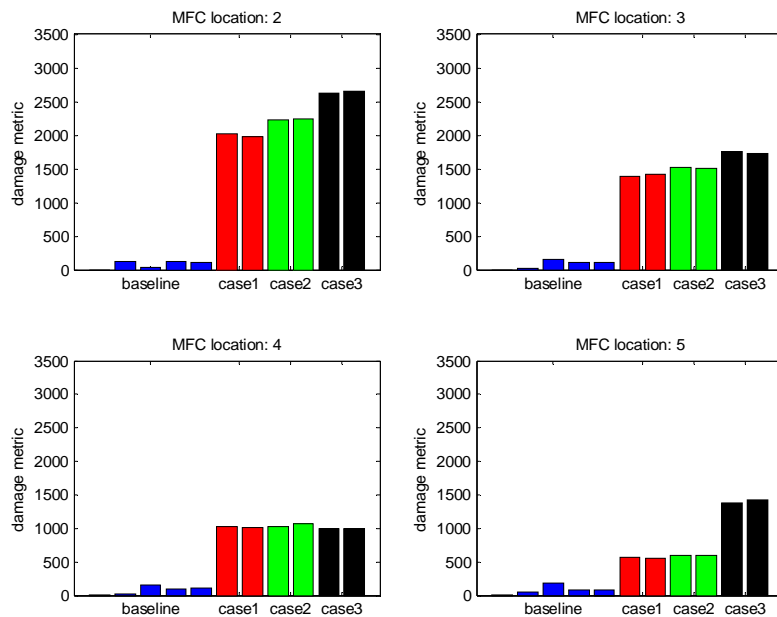


Figure 7: Impedance damage case comparison using damage metric (50 to 60-kHz)

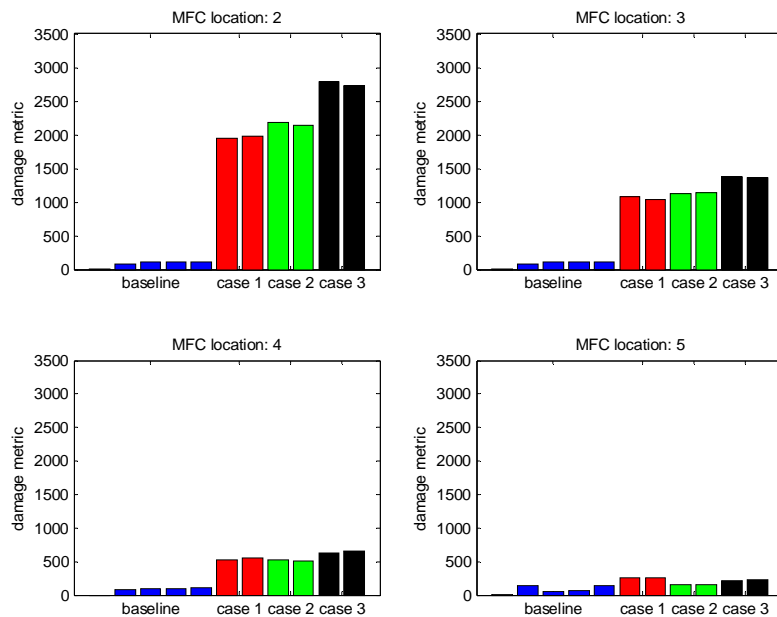


Figure 8: Impedance damage case comparison using damage metric (110 to 120-kHz)

The damage metric used here is formulated using the cross correlation coefficient between a particular damage case and the first baseline measurement. The correlation coefficient determines the linear relationship between the two data sets. The formulation of the correlation coefficient is given by the following:

$$\rho = \frac{1}{n-1} \frac{\sum_{i=1}^n (\text{Re}(Z_{i,1}) - \text{Re}(\bar{Z}_1))(\text{Re}(Z_{i,2}) - \text{Re}(\bar{Z}_2))}{\sigma_{z_1} \sigma_{z_2}} \quad (1)$$

where ρ is the correlation coefficient, $Z_{i,1}$ is the baseline impedance data and $Z_{i,2}$ is the compared impedance at frequency i , \bar{Z}_1 and \bar{Z}_2 are the means of the signals and the σ terms are the standard deviations. For convenience, the feature examined in this case is typically $(1 - \rho)$, which is done merely to ensure that the damage metric values increase with increasing damage or with increasing change in structural integrity. Therefore, a damage metric value of zero, when compared to a baseline measurement, corresponds to perfect correlation. Perfect correlation between a given measurement and a baseline measurement, in turn, means that there is no damage present for that given measurement. A greater damage metric value means that a certain degree of dissimilarity, with respect to a baseline measurement, is present in a particular measurement. In addition, an increase in the value of the damage metric corresponds to an increase in this dissimilarity. The goal here is to show that this dissimilarity is directly related to the amount of damage present.

The damage metric for the 50 to 60-kHz range for each of the damage cases is shown in Figure 7. Similar plots for the 110 to 120-kHz range are shown in Figure 8. All of the metric values are normalized by dividing them by mean of the five baselines, because the relative, rather than absolute value, are of concern in this study. This procedure minimizes the impact of a poor bonding condition between a MFC patch and the structure, which may cause relatively large variations in baseline and subsequent test measurements.

One can clearly see that the damage metric is effective at detecting the presence of damage in the structure. The damage metric is at least an order of magnitude greater for all damage cases than it is for any of the baseline measurements. From the plots in Figure 7 and in Figure 8, a clear decision regarding damage location and quantification can be made. The impedance measurements for both frequency ranges are effective at locating the damage in the system. MFC 2 and MFC 3 have damage metric for case 1 that is much greater than the corresponding damage metric for the baseline. Note that these two MFC's are located near the damage relative to MFC 4 and MFC 5. On the other hand, MFC 4 and MFC 5 have a damage metric for case 1 that is at relatively slight increases than the corresponding damage metric for the baseline. It should be noted that MFC 5 shows almost no relative difference between the baseline and damage measurements at 110-120 kHz. This lower value in the relative damage detected can be attributed to the MFC being located farther from the damage. From these results, it can be concluded that the higher frequency ranges show more localized effect compared to lower frequency ranges. The impedance measurements for both frequency ranges are also effective at quantifying the amount of damage in the system. In each instance, the damage metric increases in value as the corresponding level of damage increases, which can be clearly observed by the results of MFC 2. Therefore, structural joint damage can be detected, located, and somewhat quantified with the use of the impedance methods.

4.2 Lamb Wave Method

A Lamb wave response from the pipeline for the undamaged condition is shown in Figure 9. Transducers of the ring 3 generated the waveform and the adjacent transducers of the ring 1 measured the resulting responses. Although one transducer ring is capable of performing both tasks of actuation and sensing, due to hardware limitations, the experiment used two separate transducer rings for actuation and sensing. As mentioned in the previous section, the primary mode of concern in the experiment is the L(0,2) mode. The boundary reflected wave is clearly seen with a good signal-to-noise ratio. One can also notice that there are some other modes exist, however, because they are much smaller in magnitude compared to the L(0,2) mode, their effects are negligible.

When there are changes to the host structure's material and geometric properties, such as a surface crack or wall-thinning due to corrosion, a portion of the Lamb wave will be reflected from the damaged location back to the sensors. This reflection can be used to locate the damage site by measuring how long damage reflected wave travels (time of flight).

The Lamb wave responses before and after the damage are shown in Figure 10. Damage was introduced by applying two clamps at 1.04-m from flange A2. Although this condition is not real damage, it changes the local stiffness, which introduces the similar effects of structural damage. This procedure also allows repeated tests

before actually damaging the structure. As shown in Figure 10, the damage reflected wave is observed at 0.37e-3 sec compared to the baseline measurement.

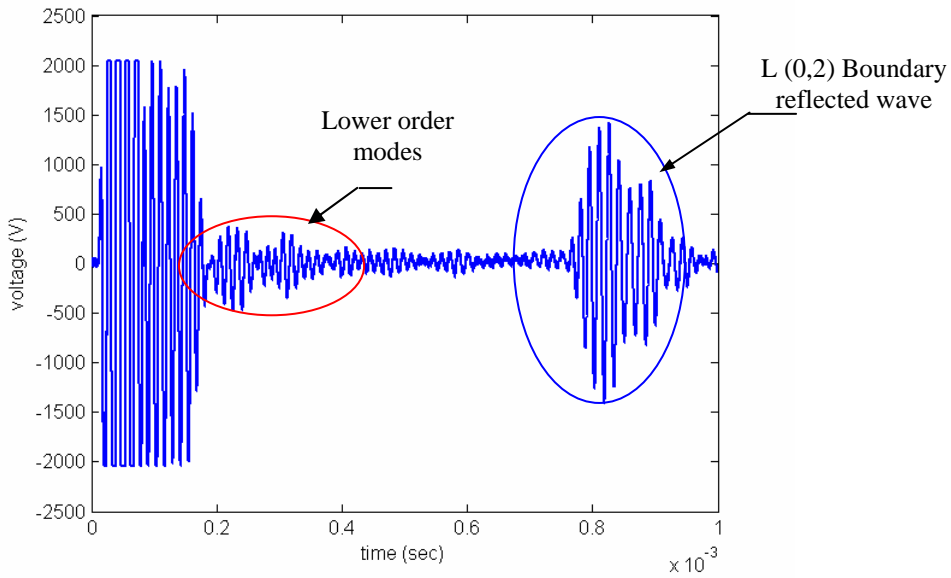


Figure 9: Lamb wave response of the undamaged case

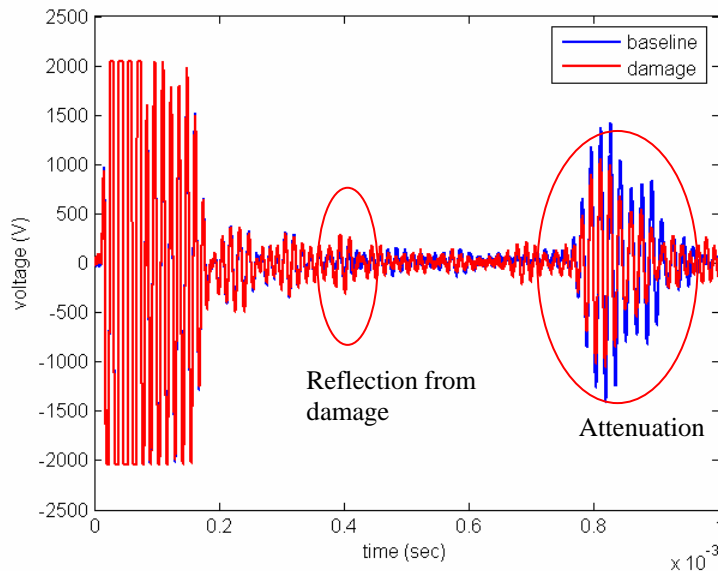


Figure 10: Reflected signals from Lamb wave testing with damaged and undamaged cases superimposed

The time of the flight for the boundary reflected wave was measured 0.76e-3 sec, yielding 5700 m/s of group velocity. Analytically, the group velocity has been estimated at 5950 m/s, as shown in Figure 1. The location of damage is, therefore, estimated at 1.022 m, which is close to the original location (1.04 m).

Because a portion of the initial signal was reflected from the damage location, the boundary reflected wave signal is expected to decrease in amplitude when compared with the baseline measurement. As shown in Figure 10,

wave attenuation from the signals reflected from the boundary is clearly observed. Therefore, both wave attenuation and reflection features could be utilized to detect and locate surface damage in pipeline structures. More advanced signal processing techniques, such as time-frequency analysis, or Wavelets, can be incorporated to automate the damage identification process, as readily available in the literature [7,8]. The magnitude of the damage reflected wave and/or the degree of attenuation of the boundary reflected wave can also be used to estimate the size or severity of surface damage.

5. DISCUSSIONS

In this study, we showed that the impedance-based and Lamb wave propagation methods can be effectively used to evaluate both joint connection and corrosion damage using the same sensors. The uniqueness of this integrated approach cannot be over-emphasized. Maintenance costs will decrease and post-event assessments can occur rapidly using the proposed approach. The entire SHM process is further simplified by application of the MFC patches to pipeline structures. The flexibility of the patches allow for direct application to the pipeline body so that the piezoelectric effect can be easily utilized. The size of the patches readily allows the MFC patches to be placed in tight or difficult to reach areas, which may not be possible with commercial transducer products requiring space for attachment.

Another important feature of this technique is that prior knowledge of a model of the system components is not necessary. This technique can be implemented at any time during the life of the system. Baseline measurements establish the initial conditions of the system and subsequent measurements can be compared to the baseline for indication that damage has occurred. Additional advantage of this technique is that the high frequency excitations affect only the local areas near the sensor. The far-field boundary conditions that make damage assessment difficult, typically encountered in low-frequency vibration methods are excluded from the measurements.

While this method demonstrated great feasibility, there are still several research issues remaining for further investigation. Although the MFC could be easily installed on the pipe, it would be somewhat labor-intensive if one needs to apply relatively large numbers of sensors and actuators to miles of pipelines. Portable instrumentation using dry-coupled MFC patches would remedy such problems. In addition, in order to maintain optimal number of sensors and actuators, the sensing region of the impedance sensor and the traveling distance of Lamb waves need to be more quantitatively assessed. The implementation of automated and more advanced signal processing techniques will improve the performance of the proposed technique. The advanced signal processing will also help to identify the severity of damage rather than just detect and locate structural damage. All of the issues mentioned here are currently being addressed and will be the subject of subsequent papers.

6. CONCLUSIONS

An integrated approach for identifying structural damage in pipeline structures has been presented. This method is based on the use of flexible MFC patches, which can be easily installed on the curved surface of the pipelines. The same MFC patches were used for both impedance-based and Lamb wave propagation methods. The impedance method was used to detect and locate connection damage in the flanged joints, in which Lamb wave methods are less sensitive. From the Lamb wave responses, the location of surface damage in main body of pipelines was identified by tracking wave attenuation and reflection information. Both methods operate at higher frequency range, where there are measurable changes in minor defects in pipeline structure. The integrated approach offers the potential for a low-cost, in-situ structural health monitoring system for pipeline structural systems.

7. ACKNOWLEDGEMENTS

The research was conducted at the Los Alamos National Laboratory, as a part of the 2004 Los Alamos Dynamics Summer School (LADSS). Funding for LADSS was provided by the Engineering Sciences & Applications Division at the Los Alamos National Laboratory and the Department of Energy's Critical Skills Programs Office. The following companies generously provided various software packages that were necessary to complete the projects: Vibrant Technologies (experimental modal analysis software), The Mathworks, Inc. (numerical analysis software), and Hibbitt, Karlsson and Sorensen, Inc. (ABAQUS finite element software). The authors would also like to acknowledge Dr. Charles Farrar, the director of LADSS, for organizing the School and providing his expert advice on this project.

REFERENCES

- [1] National Transportation Safety Board, (2000). "Natural Gas Pipeline and Fire Near Carlsbad, New Mexico, August 19, 2000" *Pipeline Accident Report NTSB/PAR-03/01*, 1-57, Washington, D.C.
- [2] National Transportation Safety Board, (1999). "Pipeline Rupture and Subsequent Fire in Bellingham, Washington, June 10, 1999" *Pipeline Accident Report NTSB/Par-02/02*, 1-79, Washington, D.C.
- [3] Posakony, G.J., Hill, V.L., (1992). "Assuring the Integrity of Natural Gas Transmission Pipelines." *Topical Report, GRI*, Nov. 1992.
- [4] Park, G., Sohn, H., Farrar, C.R., Inman, D.J. (2003). "Overview of Piezoelectric Impedance-based Health Monitoring and Path Forward," *The Shock and Vibration Digest*, **35**, 451-463.
- [5] Giurgiutiu, V., Zagrai, A., Bao, J.J. (2002). "Piezoelectric Wafer Embedded Active Sensors for Aging Aircraft Structural Health Monitoring," *International Journal of Structural Health Monitoring*, **1**, 41-61.
- [6] Bhalla, S., Soh, C.K., (2004). "High Frequency Piezoelectric Signatures for Diagnosis of Seismic/Blast Induced Structural Damages," *NDT&E International*, **37**, 23-33.
- [7] Kessler, S.S., Spearing, S.M., Soutis, C., (2002). "Damage Detection in Composite Materials using Lamb Wave Methods," *Smart Materials and Structures*, **11**, 269-278
- [8] Ihn, J.B., F.K. Chang, F.K., (2004). "Detection and monitoring of hidden fatigue crack growth using a built-in piezoelectric sensor/actuator network: II. Validation using riveted joints and repair patches," *Smart Materials and Structures*, **13**, 621-630.
- [9] Giurgiutiu, V., Zagrai, A., Bao, J.J., (2004). "Damage Identification in Aging Aircraft Structures with Piezoelectric Wafer Active Sensors," *Journal of Intelligent Material Systems and Structures*, **15**, 673-688.
- [10] Wait, J.R., Park, G., Farrar, C.R., (2004). "Integrated Structural Health Assessment using Piezoelectric Active Sensors," *Shock and Vibration*, accepted for publication.
- [11] W.K. Wilkie, R.G. Bryant, J.W. High, R.L. Fox, R.F. Hellbaum, A. Jalink, B.D. Little, and P.H. Mirick, "Low-Cost Piezocomposite Actuator for Structural Control Applications," Proceedings of 7th SPIE International Symposium on Smart Structures and Materials, Newport Beach, CA, March 5-9, 2000.
- [12] Sodano, H.A., Park, G., Inman, D.J., 2004, "An Investigation into the Performance of Macro-Fiber composites for Sensing and Structural Vibration Applications," *Mechanical Systems and Signal Processing*, **18**, 683-697.
- [13] Park, G., Farrar, C.R., Rutherford, C.A., Robertson, A.N., 2004, "Piezoelectric Active Sensor Self-diagnostics using Electrical Admittance Measurements," *ASME Journal of Vibrations and Acoustics*, submitted.
- [14] Sun, F P., Chaudhry, Z., Liang, C., Rogers, C.A. (1995), "Truss Structure Integrity Identification Using PZT sensor-actuator." *Journal of Intelligent Material Systems & Structures*, **6**, 134-139.
- [15] Park, G., Cudney, H.H. Inman, D.J. (2000) "Impedance-Based Health Monitoring of Civil Structural Components." *Journal of Infrastructure Systems*, **6**, 153-160.
- [16] Lowe, M.J.S., Alleyne, D.N., Cawley, P. (1998). "Defect Detection in Pipes Using Guided Waves." *Ultrasonics*, **36**, 147-154.
- [17] Silk, M. G., Bainton, K.F. (1979) "The propagation in metal tubing of ultrasonic wave modes equivalent to Lamb waves." *Ultrasonics*, **27**, 11-19.
- [18] Alleyne, D. N., Lowe, M., Cawley, P. (1998). "The Reflection of Guided Waves From Circumferential Notches in Pipes." *Journal of Applied Mechanics*, **65**, 635-641.
- [19] Demma, A., Cawley, P., Lowe, M., Roosenbrand, A.G. (2003). "The Reflection of the Fundamental Torsional Mode from Cracks and Notches in Pipes." *Journal of Acoustic Society of America*, **114**, 611-625.
- [20] Alleyne, D.N., Pavlakovic, B., Lowe, M., Cawley, P. (2001) "Rapid long-range inspection of chemical plant pipework using guided waves." *Insight*, **43**, 93-96.
- [21] Lowe, M., Alleyne, D.N., Cawley, P. (1998). "The Mode Conversion of a Guided Wave by a Part-Circumferential Notch in a Pipe." *Journal of Applied Mechanics*, **65**, 649-656.
- [22] Seco, F., Martin, J.M. Jimenez, A., Pons, J.L, Calderon, L., and Ceres, R. "PCDISP: A Tool for the Simulation of Wave Propagation in Cylindrical Waveguides." Proceedings of ninth International Congress on Sound and Vibration, Orlando, Florida (2002).